

AN ABSTRACT OF THE THESIS OF
Daniel Y.C. Cheung for the degree of Honors Baccalaureate of Science in Bioengineering
presented on July 26, 2013. Title: Structural and activity characterization of irradiated
antimicrobial peptide (WLBU2) for use in blood processing and biomedical applications.

Abstract approved:

Dr. Karl F. Schilke

Sepsis is a life-threatening blood infection which leads to an uncontrolled systemic inflammatory state. In North America alone, sepsis annually afflicts approximately 750,000 individuals and kills 38-50% of these (more than HIV/AIDS, breast cancer, and colon cancer combined). Current treatment involves administration of IV fluids, antibiotics and hemoperfusion, requiring prolonged ICU/hospital stays. High-throughput microfluidic devices have been proposed to remove the circulating endotoxin and pathogens from blood. A coating based on polyethylene oxide (PEO)-based triblock copolymers will prevent protein adsorption and cell adhesion. Engineered cationic amphiphilic peptides (WLBU2) tethered on the PEO chains are expected to bind circulating endotoxin and inactivate Gram-positive and Gram-negative bacterial cells. These PEO-triblock tethers will be most economically immobilized on device surfaces using γ -irradiation, and immobilization of pre-formed WLBU2-triblock constructs would greatly simplify the coating process. However, the effect of irradiation on the structure and antimicrobial activity of WLBU2 was previously unknown. In this work, we used proton nuclear magnetic resonance ($^1\text{H-NMR}$), ultraviolet (UV) spectroscopy, fluorescence spectroscopy, and circular dichroism (CD), and mass spectrometry to characterize chemical and structural changes caused by γ -irradiation. The bioactivity of γ -irradiated WLBU2 was also tested against *Escherichia coli* and *Pediococcus pentosaceus* in a radial diffusion bacterial inhibition assay. Irradiation of WLBU2 appears to cause

oxidative ring-opening of the tryptophan side-chains and a decrease in α -helicity.

However, the irradiated peptide was no less effective at inhibiting the growth of *E. coli* and *P. pentosaceus* than native WLBU2. These results suggest that using γ -irradiation to immobilize pre-formed WLBU2-triblock constructs will not destroy the antimicrobial activity of the complex and thus offers an economically viable and highly efficient means to impart biocompatibility and bioactivity in microfluidic devices.

Key words: WLBU2, AMP, antimicrobial peptide, CAP, cationic antimicrobial peptide, sepsis

Corresponding e-mail address: cheungnation@gmail.com

©Copyright by Daniel Y.C. Cheung
July 26, 2013
All Rights Reserved

Structural and activity characterization of irradiated antimicrobial peptide (WLBU2) for
use in blood processing and biomedical applications

by

Daniel Y.C. Cheung

A PROJECT

Submitted to

Oregon State University

University Honors College

in partial fulfillment of

the requirements for the

degree of

Honors Baccalaureate of Science in Bioengineering (Honors Associate)

Presented on July 26, 2013

Commencement June 2014

Honors Baccalaureate of Science in Bioengineering project of Daniel Y.C. Cheung
presented on July 26, 2013.

APPROVED:

Mentor, representing Chemical, Biological, and Environmental Engineering

Committee Member, representing Chemical, Biological, and Environmental Engineering

Committee Member, representing Chemical, Biological, and Environmental Engineering

Head, School of Chemical, Biological, and Environmental Engineering

Dean, University Honors College

I understand that my project will become part of the permanent collection of Oregon State University, University Honors College. My signature below authorizes release of my project to any reader upon request.

Daniel Y.C. Cheung, Author

ACKNOWLEDGEMENTS

I would like to thank my mentor, Dr. Karl Schilke, for guiding me through this project and for helping me develop as an engineer and scientist. I would also like Dr. Joe McGuire, Matthew Ryder, and Xiangming (Kain) Wu for training me and helping me in experimental matters; Dr. Kari Van Zee, Dr. Gombart, and Mary Fantacone for teaching me techniques and lending their lab space; Katie Watkins-Brandt and Baek Soo “Peggy” Lee for their collective help on the spectrofluorometer; Greg McKelvey for synthesizing NFK; and Gershon Starr for providing additional data for comparison. Lastly, I want to acknowledge the University Honors College for the DeLoach Work Scholarship and the Oregon State University for the Undergraduate Research, Innovation, Scholarship and Creativity award to support this work.

TABLE OF CONTENTS

| | |
|---|----|
| Introduction..... | 1 |
| WLBU2 as an antimicrobial agent for sepsis | 2 |
| Prevention of protein and cellular adsorption via copolymer triblocks | 3 |
| Linking WLBU2 to triblocks | 5 |
| Irradiated products of WLBU2 | 6 |
| Statement of Purpose | 8 |
| Materials and Methods..... | 9 |
| Proton NMR spectroscopy | 9 |
| UV spectroscopy | 9 |
| Fluorescence spectroscopy..... | 10 |
| CD spectroscopy | 10 |
| Synthesis of NFK..... | 10 |
| Fluorescence assay for NFK in γ -WLBU2 | 11 |
| Mass spectrometry | 11 |
| Radial diffusion bacterial inhibition assay..... | 12 |
| Results and Discussion | 14 |
| Structural Characterization | 14 |
| $^1\text{H-NMR}$ | 14 |
| UV spectroscopy | 15 |
| Tryptophan intrinsic fluorescence | 17 |
| Circular dichroism..... | 18 |
| Verification of NFK synthesis | 21 |
| Detection of NFK in γ -WLBU2 | 24 |
| Mass spectrometry of peptides..... | 25 |
| Antimicrobial Activity | 27 |
| Conclusions and Future Recommendations..... | 30 |
| References..... | 32 |
| Appendices..... | 35 |
| Appendix I – Reference $^1\text{H-NMR}$ Spectra..... | 36 |
| Appendix II – Radial diffusion inhibition assay plating recipe | 39 |

LIST OF FIGURES

| | |
|--|----|
| 1. Protein or cell adsorption and adhesion on a hydrophobic and hydrophilic surfaces, leading to denaturation, clots, and aggregation over time..... | 2 |
| 2. (Left) Helical form of WLBU2 shown with charged and nonpolar faces. (Right) Top-down view of the α -helix wheel of WLBU2. The positively-charged and hydrophobic side-chains are on opposing sides of the helix. | 3 |
| 3. Immobilized copolymer triblocks on a surface, forming a pendent PEO brush layer that prevents protein or cell adsorption to surfaces via steric hindrance or formation of a hydration barrier..... | 4 |
| 4. Structure of the PEO/PBD/PEO polymer triblock (Hillmyer triblock). | 5 |
| 5. Schematic of linking WLBU2 to PEO/PBD/PEO triblock in solution via chemical conjugation (top) and using γ -radiation to crosslink the WLBU2-triblock constructs to a surface (bottom)..... | 6 |
| 6. Schematic of the radial diffusion assay. | 13 |
| 7. $^1\text{H-NMR}$ result comparing WLBU2 (top) and γ -WLBU2 (bottom). Large signal peaks at 0 and 4.8 represent the reference and H_2O , respectively. Arginine and valine signals were approximately the same from 0 to 6 ppm. Loss of the signal associated with tryptophan (7 to 7.6 ppm) indicates a chemical change associated with changes in the indole ring structure..... | 15 |
| 8. Reference peak assignments for peaks between 7 – 8 ppm..... | 15 |
| 9. UV spectra of 0.3 mg/mL WLBU2 and γ -WLBU2 in water. The characteristic Trp absorbance peak at 280 nm was observed in the native WLBU2 spectrum. The absorbance peak was absent in the γ -WLBU2 spectrum, but the absorbance intensity was approximately the same. | 17 |
| 10. UV spectra of poly-L-arginine in water at different concentrations..... | 17 |
| 11. Fluorescence spectra of 0.3 mg/mL WLBU2 and γ -WLBU2 in water at excitation wavelength of 270 nm. The characteristic tryptophan emission peak at 350 nm was present in the WLBU2 spectrum but absent in γ -WLBU2 spectrum. | 18 |
| 12. CD spectra of peptides in water. Both samples exhibit expected disordered (“random coil”) properties in water, although γ -WLBU2 was less disordered than WLBU2 (decreased ellipticity). | 19 |
| 13. CD spectra of samples in different concentrations of HClO_4 . Higher HClO_4 concentration was expected to induce higher helicity, which was observed with WLBU2 (12.3% in 0.5 M HClO_4 and 9.4% in 0.2 M HClO_4). Irradiation of WLBU2 reduced its helicity under the same solution conditions (6.2% in 0.5 M HClO_4 and 7.2% in 0.2 M HClO_4). | 20 |
| 14. Reference CD spectra of different secondary structures in CD. ³⁷ | 21 |
| 15. $^1\text{H-NMR}$ spectrum of saturated NFK in DMSO- d_6 (above) in D_2O (below)..... | 22 |
| 16. UV spectrum of 0.26 mg/mL NFK. The maximum absorption peak was observed at 316 nm, close to the literature value of 318 nm. | 23 |
| 17. Fluorescence spectrum of NFK at excitation wavelength of 330 nm. The characteristic peak at 440 nm was observed, consistent with the literature value. | 23 |
| 18. Reaction scheme of the NFKPIP fluorescence assay. ²³ | 24 |

| | |
|--|----|
| 19. Fluorescence spectra of native and irradiated (A) WLBU2 and (B) WLBU2-PIP solutions at excitation wavelengths 330 nm and 400 nm, respectively. NFK has a characteristic emission peak at 400 nm when excited at 330 nm. NFK-PIP has a reported peak at 500 nm when excited at 400 nm. Water peak at approximately 400 nm was not suppressed..... | 25 |
| 20. Low resolution mass spectrum of 0.3 mg/mL WLBU2. | 26 |
| 21. Low-resolution mass spectrum of 1.0 mg/mL γ -WLBU2. | 26 |
| 22. Radial diffusion bacterial inhibition assay results of <i>E. coli</i> (top row) and <i>P. pentosaceus</i> (bottom row). Numbering scheme corresponds to Table 2. | 28 |
| 23. Mean diameter of WLBU2 kill zones against <i>E. coli</i> and <i>P. pentosaceus</i> . A small effect of concentration was observed. Deuterated water (D ₂ O) had no effect on bacterial inhibition, with or without WLBU2 peptide. Error bars represent 95% confidence interval (N = 3). | 29 |

LIST OF TABLES

1. Major irradiated products of tryptophan after 3 kGy from most abundant to least abundant: NFK, OIA, OH-Trp isomers, and KYN.7
2. List of solutions and concentrations used for the radial diffusion bacterial inhibition assay.28

LIST OF APPENDICES FIGURES

1. Figure AI 1. Reference ^1H -NMR spectrum of L-arginine in D_2O with peak assignments.36
2. Figure AI 2. Reference ^1H -NMR spectrum of L-tryptophan in H_2O with peak assignments.....37
3. Figure AI 3. Reference ^1H -NMR spectrum of DL-valine in D_2O with peak assignments.38

Introduction

Sepsis is a potentially deadly condition that is characterized by a whole-body inflammatory state in response to systemic bacterial infections that afflicts approximately 750,000 individuals and kills 215,000 in North America annually (more than breast cancer, colon cancer, and HIV/AIDS combined)¹, costing an estimated \$17 billion per year to treat.² Gram-negative bacteria cell wall consists of lipopolysaccharides (LPS) or endotoxins, which, when released by cell lysis, cause an overwhelming response of the body to fight the infection, triggering inflammation throughout the body. Gram-positive bacteria release exotoxins that intensify the immune response to LPS.³ Prolonged exposure to the toxins without treatment will eventually result in organ failure, leading to death.

Current treatment involves administration of IV fluids, antibiotics, vasopressors, and other medications, but the time spent in the hospital average nearly 20 days.⁴ Therefore, a microfluidic device coated with antimicrobials has been proposed to process blood to filter out pathogens causing sepsis. Although the high surface area-to-volume ratio in the microchannels offers opportunities to effectively clear the body's blood volume, the channels are susceptible to air bubble formation, blood clotting, or protein aggregation via surface-protein interactions (Figure 1). Formation of a pathogenic biofilm layer via adsorption decreases the device efficacy and prolongs healing time, which increases costs for patients. Devices coated with an anti-fouling, bioactive layer should prevent protein and cell adsorption while maximizing capture and kill against bacteria and other pathogens present.

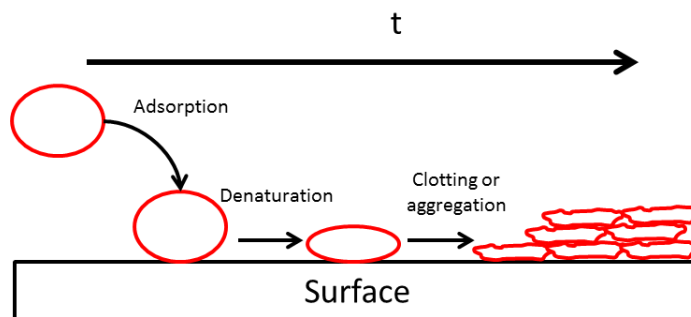


Figure 1. Protein or cell adsorption and adhesion on a hydrophobic and hydrophilic surfaces, leading to denaturation, clots, and aggregation over time.

WLBU2 as an antimicrobial agent for sepsis

Cationic antimicrobial peptides (CAPs) are peptides with secondary structures that have positively-charged and hydrophobic side-chains segregated on opposing sides of the helix that disrupt the negatively-charged bacterial phospholipid membrane, thereby killing the pathogens physically without increasing antibiotic resistance.⁵ These peptides are present in many organisms and act as natural antibiotics by either directly killing pathogens or modulating innate immune response, making them an excellent template to mimic for new anti-infective therapeutic strategies.² The ideal CAP would have broad activity spectra, killing Gram-positive and Gram-negative bacteria, fungi, viruses, and even parasites. Unfortunately, most CAPs are not selective against many pathogens, and many factors affect the efficacy of CAPs, including sensitivity to physiological conditions (e.g. presence of cations like K^+ , Na^+ , Ca^{2+} , and Mg^{2+}). One other important consideration when evaluating CAPs is their potential toxicity to mammalian cells.

WLBU2, however, has been shown to overcome these challenges. WLBU2 (RRWVRRVRRWVRRVVRVRRWVRR, 3.4 kDa) is an engineered, amphipathic CAP that in α -helical form is composed of a polar face (13 arginine residues) and a nonpolar

face (8 valine and 3 tryptophan residues) (Figure 2).^{6,7} It is also an analogue of the human cathelicidin peptide LL-37, which also has broad antimicrobial activity and neutralizes LPS, but WLBU2 outperforms LL-37 in physiological settings.^{6,7} The residues of the peptide have been engineered to maximize helicity and tryptophan content, conferring to greater antimicrobial potency. The peptide has been shown to bind and kill Gram-positive (*Staphylococcus aureus*) and Gram-negative (*Pseudomonas aeruginosa*) bacteria in human serum without damaging mammalian cells.^{7,8} These attributes make WLBU2 a viable option for use in blood processing applications.

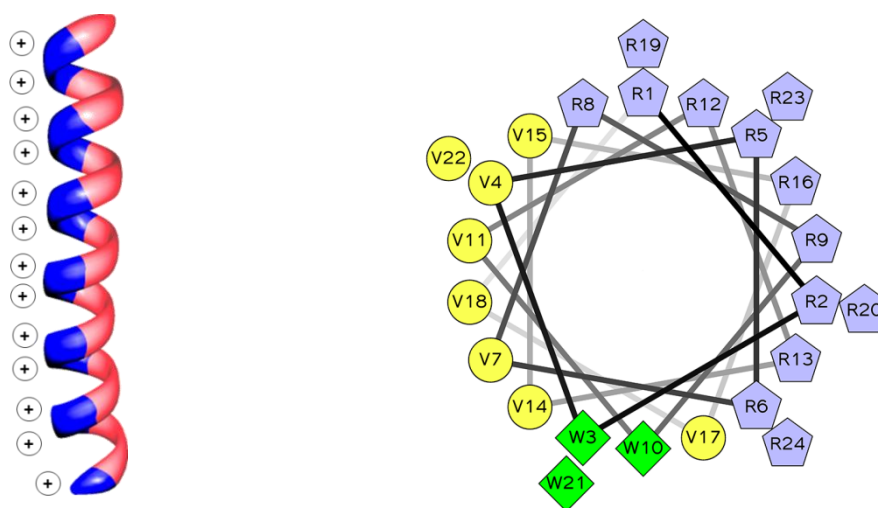


Figure 2. (Left) Helical form of WLBU2 shown with charged and nonpolar faces. (Right) Top-down view of the α -helix wheel of WLBU2. The positively-charged and hydrophobic side-chains are on opposing sides of the helix.

Prevention of protein and cellular adsorption via copolymer triblocks

Copolymer triblocks are composed of two hydrophilic tails covalently linked to a hydrophobic center block, which is used to attach to hydrophobic surfaces. In the well-characterized, commercially important Pluronics[®] triblock family, poly(ethylene oxide) (PEO) and poly(propylene oxide) (PPO) are used as the hydrophilic side chains and hydrophobic center, respectively.⁹ Previous studies have shown that surfaces coated with

copolymer triblocks prevent protein adsorption and cell adhesion via steric repulsion by formation of a pendant brush layer (Figure 3).⁹⁻¹¹ The triblocks readily self-assemble onto hydrophobic surfaces from aqueous solutions via the hydrophobic association between the PPO center block and the surface.¹²

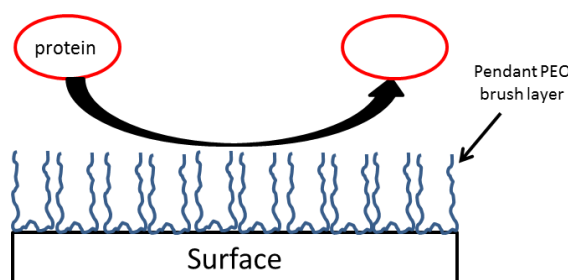


Figure 3. Immobilized copolymer triblocks on a surface, forming a pendent PEO brush layer that prevents protein or cell adsorption to surfaces via steric hindrance or formation of a hydration barrier.

One limitation of immobilizing Pluronic[®] triblocks on hydrophobic surfaces is the competitive elution of the triblocks by blood proteins.¹³ One option to overcome this limitation is to use poly(butadiene) (PBD) as the center block, which contains vinyl groups. Past research has shown grafting of Pluronic[®] triblock by γ -irradiation (3 kGy) on trichlorovinylsilane (TVCS)-treated surfaces.¹⁴ The vinyl groups on TVCS are activated upon γ -irradiation, forming free radicals to attack the adsorbed PPO portion of the triblock, thus grafting the surfactant onto the surface via covalent bonds.¹⁴ Using the same concept, the vinyl groups in PBD can be activated via γ -irradiation and used to covalently link the triblock to polymer surfaces, potentially making PBD a better choice for blood processing applications. The vinyl-containing polymer triblocks (Hillmyer triblocks) have a general chemical formula of $(\text{PEO})_n\text{-(PBD)}_m\text{-(PEO)}_n$, where n and m are the number of repeating units (Figure 4).

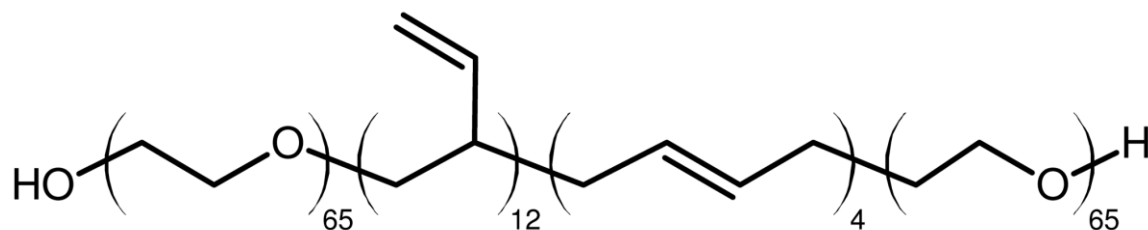


Figure 4. Structure of the PEO/PBD/PEO polymer triblock (Hillmyer triblock).

Linking WLBU2 to triblocks

Previous research has demonstrated covalently linking heparin to F108-based triblocks (end-group activated Pluronic[®], EGAP) as a method to block protein aggregation and prevent clotting.¹⁵ Using the same concept, the novel antimicrobial peptide WLBU2 is a promising candidate for attaching on the PEO as an antimicrobial because of its ability to bind and kill bacteria and its nontoxicity to mammalian cells. One commercially viable and effective method to create an anti-infective surface coating is through immobilization of synthetic constructs of PEO-based triblock copolymers (PEO/PBD/PEO) and WLBU2 and using γ -radiation to crosslink the WLBU2-triblock constructs to the surface (Figure 5). However, the effect of γ -irradiation on the structure and activity of WLBU2 was unknown. If irradiation negatively impacts the peptide by decreasing the killing and binding activity, then another approach must be used to immobilize the WLBU2-triblock constructs.

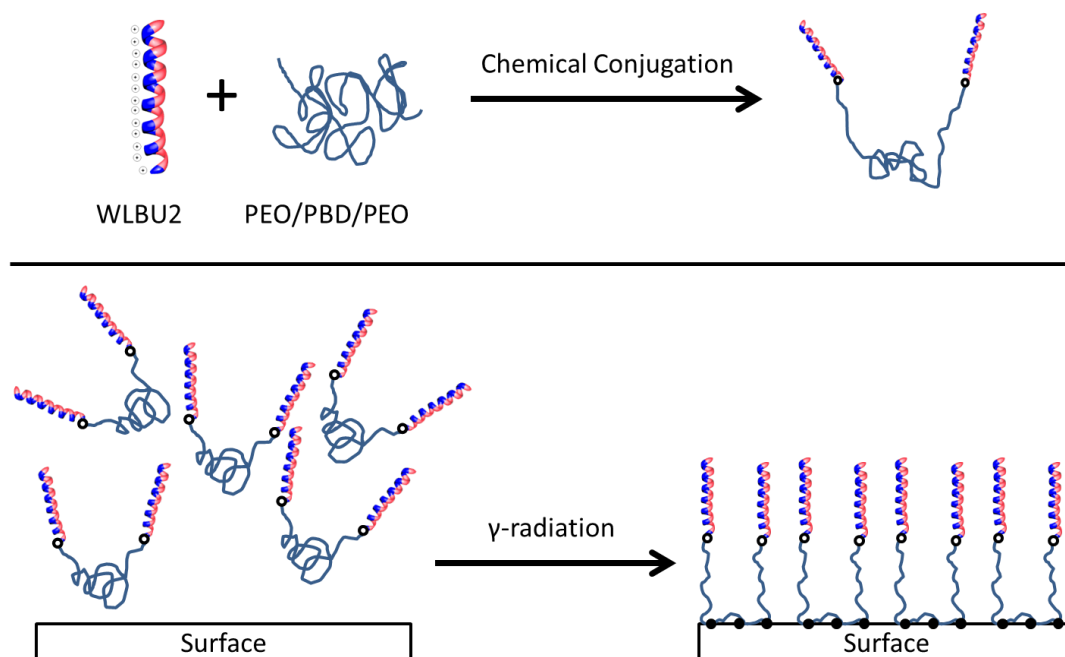


Figure 5. Schematic of linking WLBu2 to PEO/PBD/PEO triblock in solution via chemical conjugation (top) and using γ -radiation to crosslink the WLBu2-triblock constructs to a surface (bottom).

Irradiated products of WLBu2

Amino acids undergo a variety of reactions with radicals in aqueous solution, mainly with hydroxyl radicals ($\cdot\text{OH}$), which possess strong oxidative properties.¹⁶ The most reactive amino acids contain aromatic rings (Trp, Tyr, His) and sulfur groups (Met, Cys), and the least reactive is glycine.¹⁶ In WLBu2, the order of reactivity via radiolysis from most reactive to least is tryptophan, arginine, and valine.¹⁷ Therefore, the highly reactive tryptophan in WLBu2 could be a source for structural change upon γ -irradiation. Major oxidative products of γ -irradiated aqueous tryptophan solutions after 3 kGy are listed in Table 1, with *N*-formylkynurenine (NFK) being the major product, followed by oxindolylalanine, the four OH-tryptophan isomers, and kynurenine.¹⁸ However, the major oxidative products listed only account for a small percentage of all the possible irradiated products, with the remaining molecules not yet elucidated.¹⁸ In lower concentrations of

tryptophan, percentage of tryptophan destruction and formation of major oxidative products are increased.¹⁸

Table 1. Major irradiated products of tryptophan after 3 kGy from most abundant to least abundant: NFK, OIA, OH-Trp isomers, and KYN.

| | |
|-------------------------------|---------------------------------|
| <p>Oxindolylalanine (OIA)</p> | <p>Kynurenine (KYN)</p> |
| <p>OH-Trp (4, 5, 6, 7)</p> | <p>N-formylkynurenine (NFK)</p> |

Statement of Purpose

The characterization of irradiated WLBU2 (γ -WLBU2) addressed the feasibility of immobilizing the preformed WLBU2-PEO/PBD/PEO triblock constructs on polymer medical device surfaces. It was hypothesized that irradiation will cause structural changes to WLBU2 by oxidizing the tryptophan ring without hindering its activity to bind and kill bacteria. The project compared spectra of irradiated WLBU2 against non-irradiated WLBU2 to observe any changes via proton nuclear magnetic resonance, ultraviolet, fluorescence, and circular dichroism spectroscopies. Deviation from the standard spectrum indicates a change in structure. The bioactivity of γ -irradiated WLBU2 was assessed with radial diffusion bacterial kill assay and quantified by the kill zone area.

Materials and Methods

Lyophilized WLBU2 was purchased from Genscript (Piscataway, NJ). HPLC-grade water and deuterated water (D₂O) were used to make stock WLBU2 solutions at 5 mg/mL. All other materials and reagents used were analytical or better grade. Solutions were aliquoted and diluted to 0.3 and 1.0 mg/mL with water and irradiated to 3 kGy by a ⁶⁰Co source. All samples were stored at 4 °C.

Proton nuclear magnetic resonance (¹H-NMR), ultraviolet (UV) spectroscopy, mass spectrometry, and circular dichroism (CD) spectroscopy were used to analyze the structure of the irradiated peptide. The activity of WLBU2 and γ -irradiated WLBU2 was tested against *Escherichia coli* (DH5 α) (Gram-negative) and *Pediococcus pentosaceus* (Gram-positive).

Proton NMR spectroscopy

Proton nuclear magnetic resonance (¹H-NMR) spectra were taken using a Brüker (Billerica, MA) Robinson 400 MHz NMR spectrometer with TopSpin 2.1 software at room temperature (25 °C) using 1.0 mg/mL WLBU2 and γ -WLBU2 in D₂O. Each sample was measured using 128 scans. The spectra were post processed by setting the line broadening factor to 0.8 Hz.

UV spectroscopy

Ultraviolet (UV) absorbance measurement scans of peptide solutions at 0.3 mg/mL in water were taken with a Thermo Electron Corporation (Waltham, MA)

Genesys 6 ultraviolet-visible spectrophotometer at 25 °C between 200 and 400 nm at 1 nm intervals using a 1 cm UV quartz cuvette.

Fluorescence spectroscopy

Fluorescence intensity measurement scans of 0.3 mg/mL peptide solutions in water were taken using a Horiba Jobin Yvon MicroMax 384 plate reader and a Horiba Jobin Yvon (Edison, NJ) Fluorolog-3 Spectrofluorometer at an excitation wavelength of 270 nm at 25 °C with entrance and exit slits set to 2 nm.

CD spectroscopy

Circular dichroism (CD) measurements were taken with a Jasco (Easton, MD) J-815 CD spectrometer at 25 °C between 180 and 280 nm with samples in water or HClO₄ using a 10.00 mm circular QS quartz cuvette with 2 nm band width. Aliquots of WLBU2 and irradiated WLBU2 were diluted to 0.3 mg/mL in water, or 0.2 mg/mL in 0.2 M or 0.5 M HClO₄ to induce α -helix conformation.¹⁹ The ellipticity for 5 scans per experimental trial was plotted against wavelength. DichroWeb was used to deconvolute and determine the percent helicity of the samples by using the CONTIN or CDSSTR preset methods.^{20,21}

Synthesis of NFK

NFK was synthesized as a positive control using the procedure of Ehrenshaft et al.²² Acetic anhydride (1.5 mL) was mixed with formic acid (3 mL) on ice and then warmed to room temperature (25 °C). The mixture was added to kynurenine (2 g) and formic acid (4.5 mL). The sample was left overnight at 25 °C to complete the formylation

reaction. A large excess of ether was added, and the mixture was allowed to stand on ice for 1 hr. Ethanol was added (200 proof) after the ether was decanted, and the NFK was kept on ice for 1 hr. The NFK was recovered by removal of ethanol via pipetting and drying with a gentle stream of argon. The product was verified by $^1\text{H-NMR}$ and UV spectroscopies

Fluorescence assay for NFK in γ -WLBU2

The formation of *N*-formylkynurenine (NFK), one major tryptophan oxidative product upon irradiation, was measured using an assay established by Tomek et al. (PIP fluorescence assay).²³ The irradiated WLBU2 (0.3 mg/mL in water) was mixed with piperidine (PIP) (200 mM final concentration) and heated at 65 °C for 20 minutes in a water bath. The WLBU2-PIP solution fluorescence intensity was measured at 25 °C using a Horiba Jobin Yvon MicroMax 384 plate reader and a Horiba Jobin Yvon Fluorolog-3 spectrofluorometer at an excitation wavelength of 400 nm for emission at 500 nm.

Mass spectrometry

Mass spectrometry spectra of 1.0 mg/mL WLBU2 and γ -WLBU2 in water were obtained using electrospray ionization (ESI) performed by the Biomolecular Mass Spectrometry Core of the Environmental Health Sciences Core Center at Oregon State University.

Radial diffusion bacterial inhibition assay

A radial diffusion assay was performed on *Escherichia coli* and *Pediococcus pentosaceus* to semi-quantitatively analyze antimicrobial activity of irradiated WLBU2 at different concentrations. Luria broth (LB) and Lactobacilli MRS broth (Appendix II) were used to grow *E. coli* and *P. pentosaceus*, respectively, in suspended media at 37 °C overnight to at least 4×10^8 colony forming units (CFU)/mL. The optical density at 600 nm (OD_{600}) was measured via spectrophotometry and converted to CFU using the conversion factor $OD_{600} = 1 = 1 \times 10^9$ CFU.

The recipe for plating was adapted from previous studies and can found in Appendix II with the process shown in Figure 6.²⁴ The under- and over-layer solutions were heated to melt and cooled to 55 °C in a water bath. Bacteria were added to the under layer for a final concentration of 4×10^7 CFU/mL in 10 mL. The bacteria-under layer mixture was poured into plastic Petri dishes and allowed to cool. Small wells ($D = 3.3$ mm) were punched in the solidified under layer using a truncated P-1000 pipette tip. Peptide samples (6 μ L) at different concentrations were added into each well. Water and D₂O were used as negative controls, and 50 mg/mL ampicillin was used as a positive control. The solutions were allowed to diffuse into the gel for approximately 2 hours. The top layer (10 mL) was then poured on top of the plate and allowed to cool. The layered plates were incubated overnight at 37 °C. The diameter of the kill zones was measured after 24 hours.

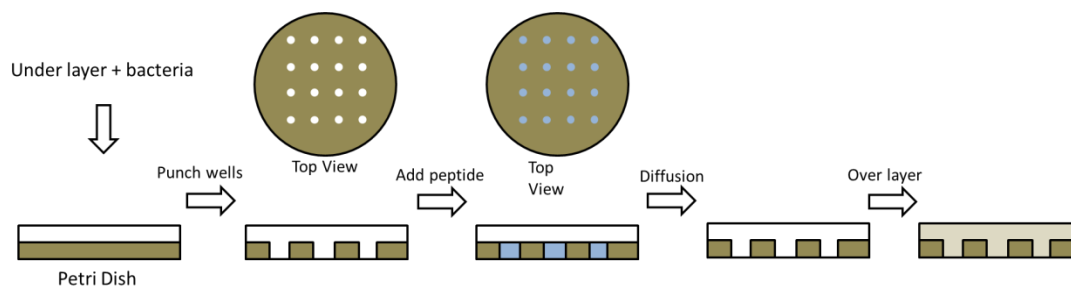


Figure 6. Schematic of the radial diffusion assay.

Kill zone quantification analysis was performed using ImageJ software.²⁵ The kill zone area was calculated by subtracting the well sizes from the measured kill zone area. The average pixel count of the 12 wells was used as a conversion factor to convert pixels to mm^2 .

Results and Discussion

Structural Characterization

¹H-NMR

Figure 7 shows the ¹H-NMR results between 0.3 mg/mL WLBU2 and γ -WLBU2. Expected peaks for each amino acid were gathered from the National Institute of Advanced Industrial Science and Technology (AIST) spectral database and the Human Metabolome Database.²⁶⁻²⁹ Reference spectra are given in Appendix I. Reference TMS and solvent (HOD) signals are shown at 0 and 4.8 ppm, respectively. All peaks associated with arginine and valine were visible in both spectra. However, the peaks associated with the indole ring structure in tryptophan ($\delta = 7.0-7.6$) in the γ -WLBU2 spectrum were absent, suggesting that the structural integrity of the tryptophan ring may have been opened during γ -irradiation. This observation is consistent with tryptophan reacting strongly with radicals, which are mostly hydroxyl radicals in water, causing oxidation of the indole ring structure. Additional tests were performed to confirm the suspected major product NFK (see sections below).

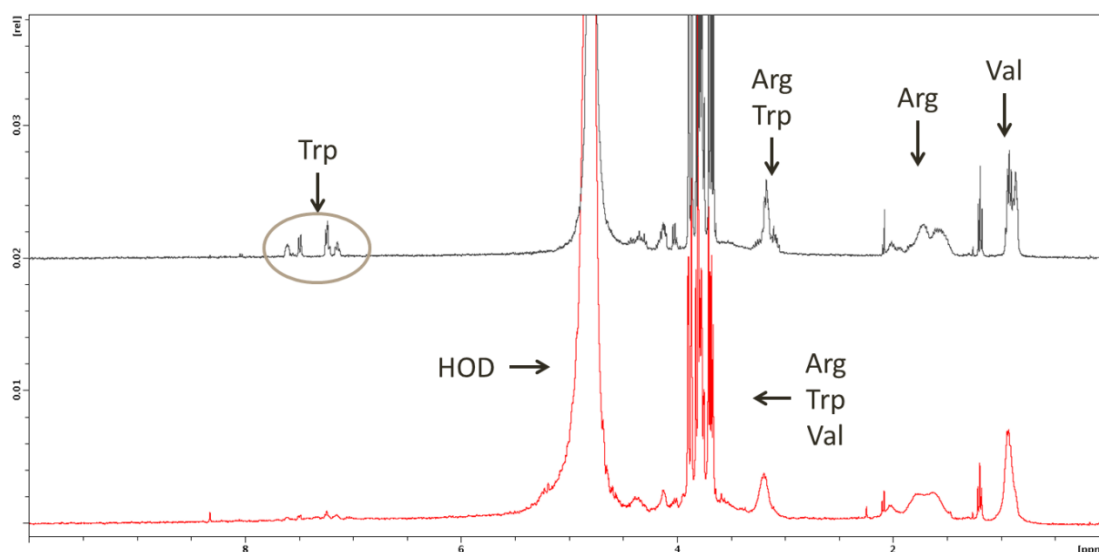


Figure 7. $^1\text{H-NMR}$ result comparing WLBU2 (top) and γ -WLBU2 (bottom). Large signal peaks at 0 and 4.8 represent the reference and H_2O , respectively. Arginine and valine signals were approximately the same from 0 to 6 ppm. Loss of the signal associated with tryptophan (7 to 7.6 ppm) indicates a chemical change associated with changes in the indole ring structure.

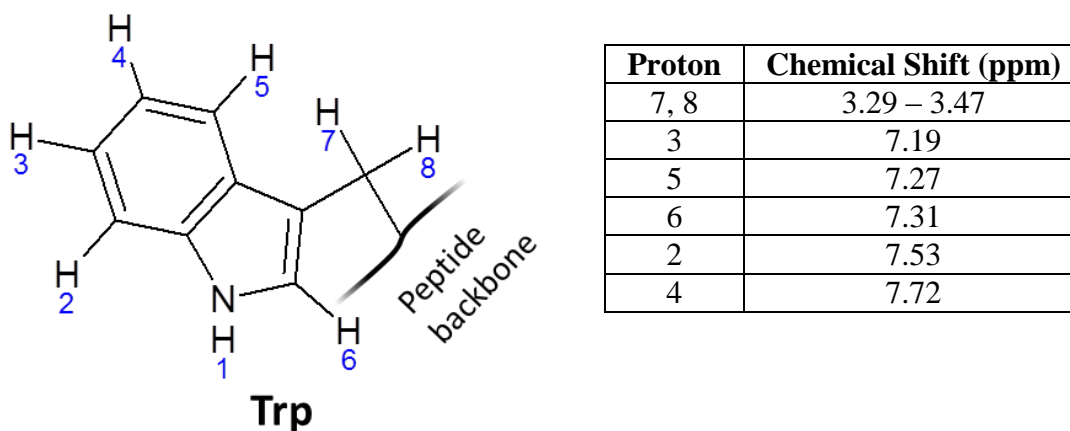


Figure 8. Reference peak assignments for peaks between 7 – 8 ppm.

UV spectroscopy

The UV spectra of 0.3 mg/mL WLBU2 and γ -WLBU2 are shown in Figure 9. The expected tryptophan absorption peak at approximately 280 nm is visible in the control

spectrum of native WLBU2.³⁰ However, the γ -WLBU2 spectrum changed drastically. Although the characteristic tryptophan peak at 280 nm was absent, which is indicative of tryptophan modification, the absorbance intensity was approximately the same. This could suggest that some tryptophan residues remained intact upon irradiation, which is consistent with previous studies.¹⁸ In addition, the pure poly-arginine spectra do not have much absorbance at 280 nm, further implying that there may be partial intact tryptophan (Figure 10). The blue-shift of the WLBU2 peak at approximately 230 nm to 210 nm could be a property of arginine, which is consistent with data collected from poly-L-arginine, but the quality of the cuvette used does not accurately read below approximately 240 nm. The differences in the spectra further suggest that a structural change occurs in WLBU2 upon γ -irradiation, which is consistent with an opening in the indole structure.

The predicted major oxidative product NFK has a characteristic absorbance peak at 318 nm³¹, which was not observed in the γ -WLBU2 spectrum. However, it is a possibility that the formation of NFK falls below the detection limit for UV spectroscopy because the irradiated products are produced in low quantities.¹⁸

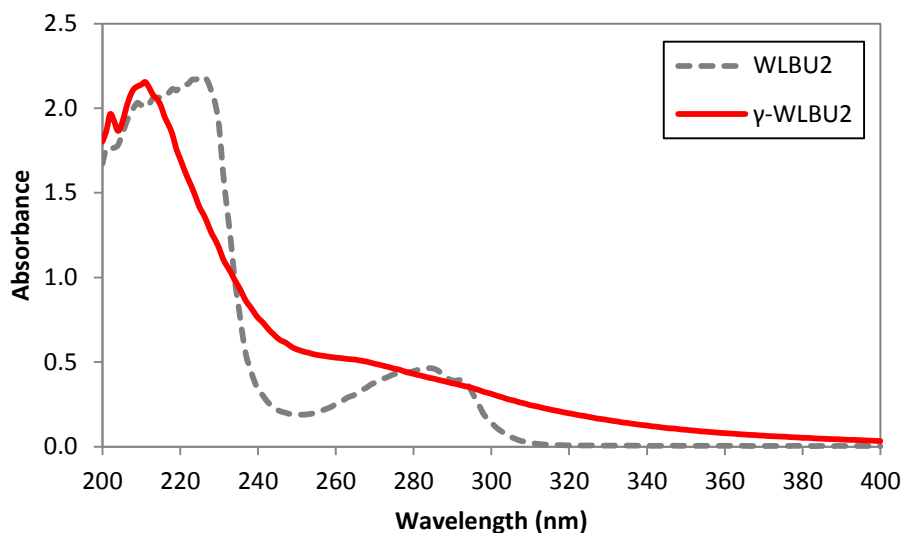


Figure 9. UV spectra of 0.3 mg/mL WLBU2 and γ -WLBU2 in water. The characteristic Trp absorbance peak at 280 nm was observed in the native WLBU2 spectrum. The absorbance peak was absent in the γ -WLBU2 spectrum, but the absorbance intensity was approximately the same.

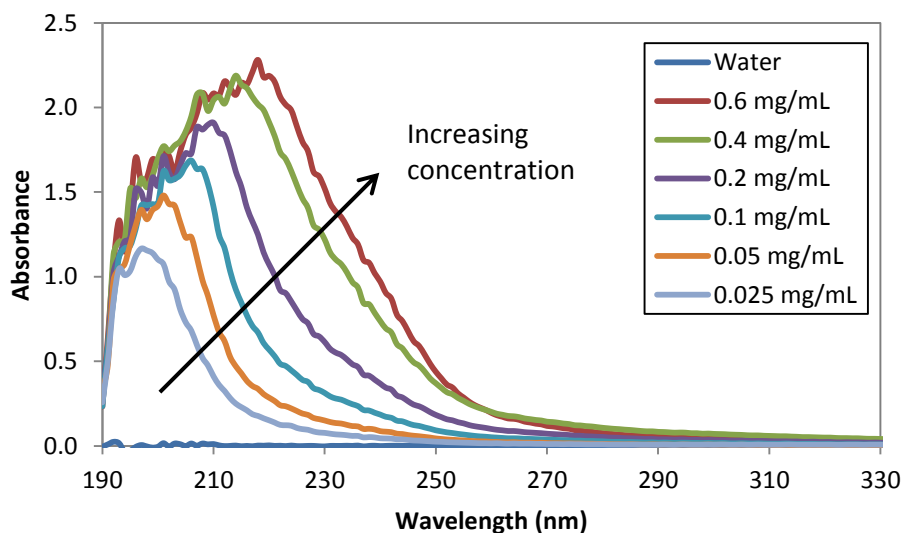


Figure 10. UV spectra of poly-L-arginine in water at different concentrations.

Tryptophan intrinsic fluorescence

The fluorescence spectra of 0.3 mg/mL WLBU2 and γ -WLBU2 in water at excitation wavelength of 270 nm are shown in Figure 11. The expected emission peak at

approximately 350 nm corresponding to tryptophan was present for WLBU2 but absent for γ -WLBU2, further suggesting that γ -irradiation modified the tryptophan side chains of WLBU2 by radical chemistry reactions with water-derived hydroxyl radicals ($\cdot\text{OH}$).³²⁻³⁴

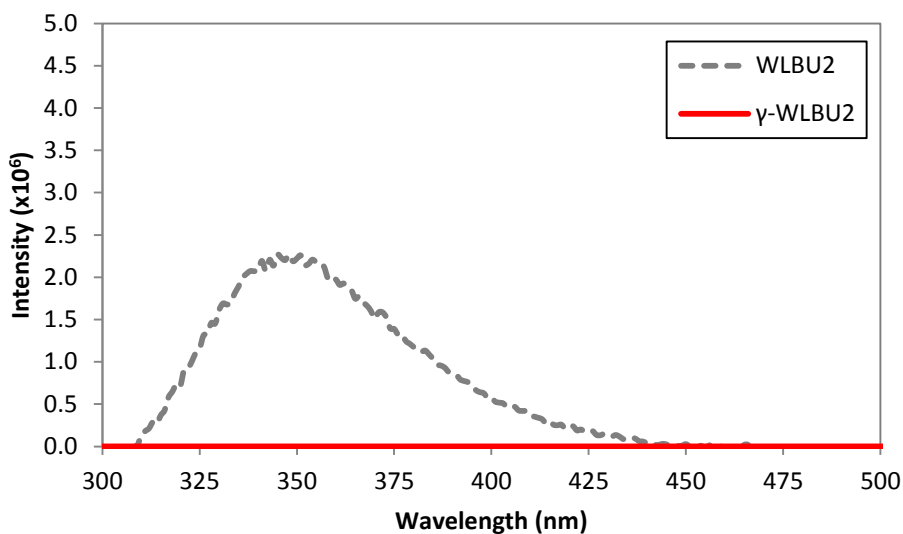


Figure 11. Fluorescence spectra of 0.3 mg/mL WLBU2 and γ -WLBU2 in water at excitation wavelength of 270 nm. The characteristic tryptophan emission peak at 350 nm was present in the WLBU2 spectrum but absent in γ -WLBU2 spectrum.

Circular dichroism

The CD spectra of 0.3 mg/mL WLBU2 and γ -WLBU2 in water is shown in Figure 12. WLBU2 in water showed little stable secondary structures, which is consistent with previous studies.³⁵ γ -WLBU2 also exhibited similar disordered (“random coil”) properties, although it was less disordered than WLBU2. The decrease in the disordered conformation could be due to the effects of the oxidized tryptophan side-chains, which are more polar than tryptophan. Both samples showed similar structural features in D_2O , implying that the choice of solvent (H_2O vs. D_2O) does not affect the peptide structure (data not shown).

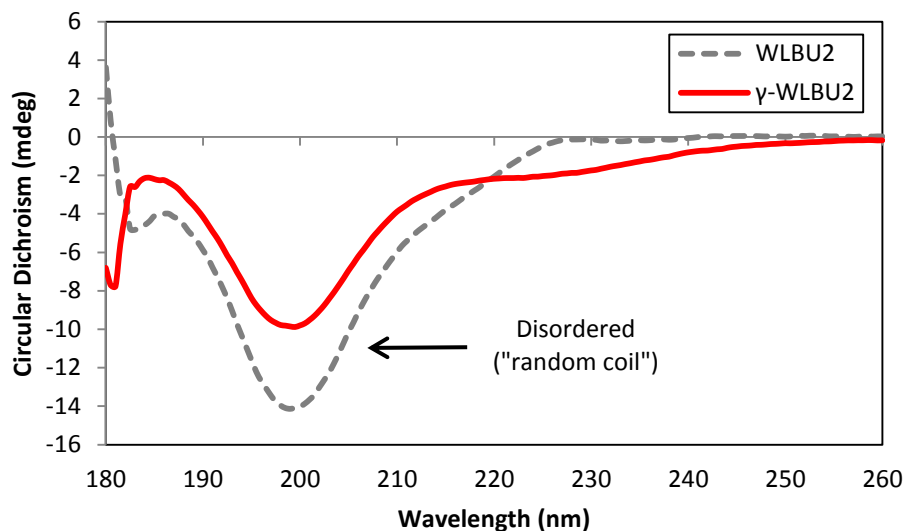


Figure 12. CD spectra of peptides in water. Both samples exhibit expected disordered (“random coil”) properties in water, although γ -WLBU2 was less disordered than WLBU2 (decreased ellipticity).

The peptides were induced to α -helical conformations by adding HClO_4 (Figure 13). Although WLBU2 in 0.2 M and 0.5 M HClO_4 displayed low α -helicity content (approximately 9.4% and 12.3%), the trends are consistent with previous data.³⁵ γ -WLBU2, however, displayed much lower helicity at the same concentrations (7.2% and 6.2% in 0.2 M and 0.5 M HClO_4 , respectively). Higher concentrations of perchlorate ion generally induce higher percentage of helicity³⁵, but this was less apparent for γ -WLBU2. The cleavage of the indole structure may have impacted its ability to remain helical in presence of perchlorate ions possibly by slightly increasing peptide’s polarity. Water molecules solvate the peptide, but perchlorate ions compete with water molecules.³⁶ The stronger ion solvation ultimately stabilizes the α -helix conformation by causing a loss of hydration in the peptide, which promotes intrapeptide hydrogen bonding.³⁶ With more polar side-chains, the interaction between γ -WLBU2 and water molecules may be more favourable, causing a weaker α -helical structure, which is consistent with the data

collected. The differences in spectra between native WLBU2 and γ -WLBU2 in HClO_4 suggest a structural change of the tryptophan side-chains to a more polar residue. A reference spectra of different secondary structures in CD from Greenfield et al. is given in Figure 14 for comparison.³⁷

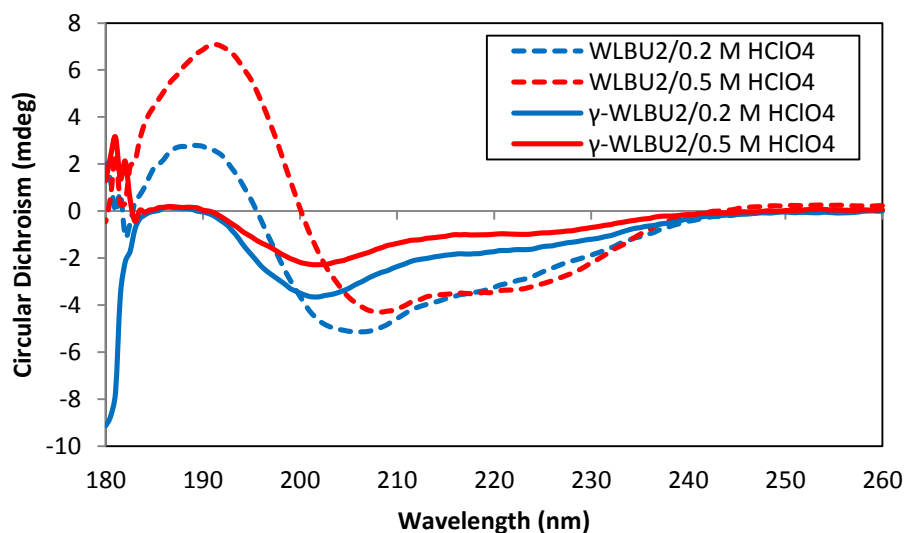


Figure 13. CD spectra of samples in different concentrations of HClO_4 . Higher HClO_4 concentration was expected to induce higher helicity, which was observed with WLBU2 (12.3% in 0.5 M HClO_4 and 9.4% in 0.2 M HClO_4). Irradiation of WLBU2 reduced its helicity under the same solution conditions (6.2% in 0.5 M HClO_4 and 7.2% in 0.2 M HClO_4).

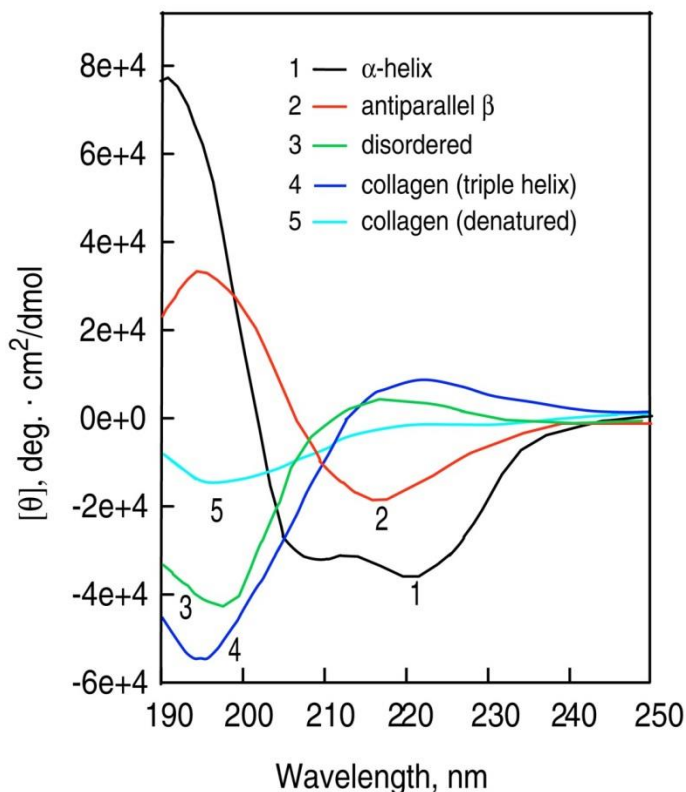


Figure 14. Reference CD spectra of different secondary structures in CD.³⁷

Verification of NFK synthesis

The ¹H-NMR spectra of the synthesized NFK in DMSO-d₆ and D₂O are shown in Figure 15. Both samples were saturated in each solvent, yet the spectra showed weak signal peaks relative to the solvent and water peaks, but the signals were not consistent with literature values^{38,39}, which suggests that the compound is either not NFK or the NFK is not pure (no reference spectrum available). Saturated NFK in CDCl₃ was also used in a separate experiment, but only solvent peaks were observed (data not shown). The UV spectrum of 0.26 mg/mL NFK is shown in Figure 16. The maximum absorption peak was observed at 316 nm, which is approximately consistent with the literature value of 318 nm.⁴⁰ The UV result, although a weaker analysis than ¹H-NMR, may suggest the synthesized compound is NFK. The fluorescence emission spectrum of NFK at excitation

wavelength of 330 nm is displayed in Figure 17. NFK has a characteristic emission fluorescence peak at 440 nm, which was observed in the spectrum.³¹ From the three spectral analysis of the synthesized compound, UV and fluorescence were not inconsistent with literature values, but the $^1\text{H-NMR}$ spectra deviated from literature values. The first two analyses used weaker techniques for structural verification of the compound than $^1\text{H-NMR}$, so the synthesized product cannot be confirmed with certainty that it is NFK.

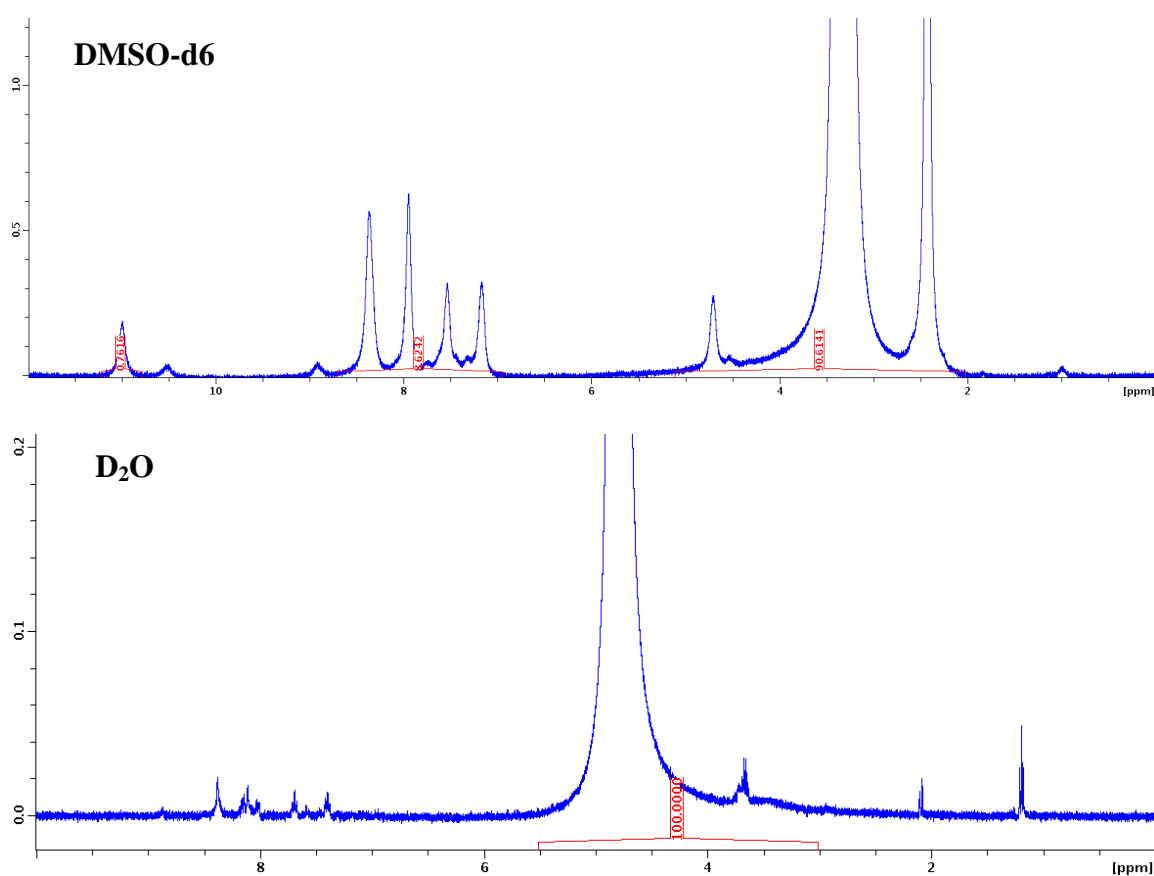


Figure 15. $^1\text{H-NMR}$ spectrum of saturated NFK in DMSO-d₆ (above) in D₂O (below)

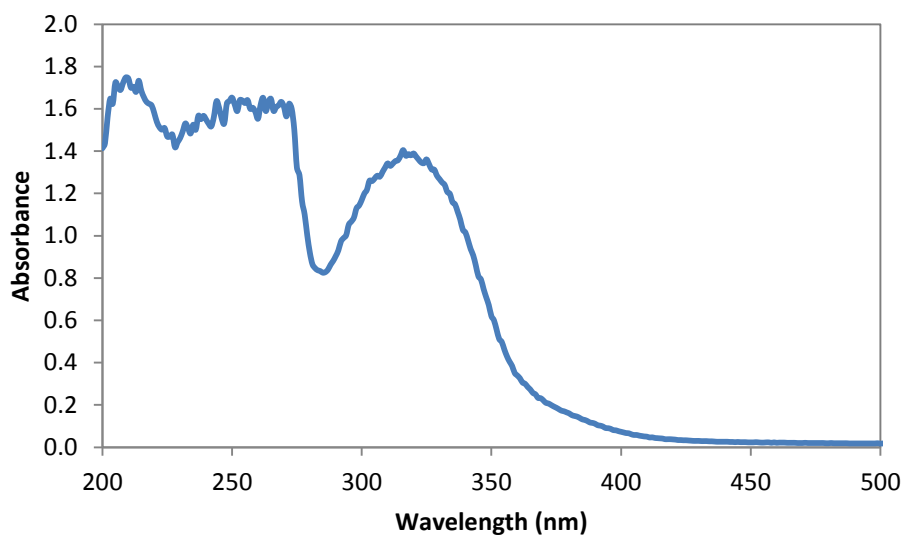


Figure 16. UV spectrum of 0.26 mg/mL NFK. The maximum absorption peak was observed at 316 nm, close to the literature value of 318 nm.

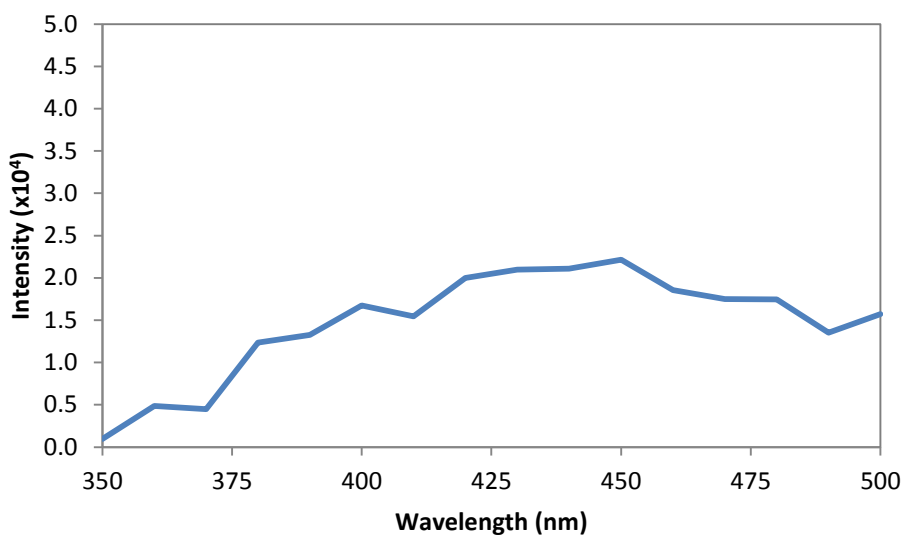


Figure 17. Fluorescence spectrum of NFK at excitation wavelength of 330 nm. The characteristic peak at 440 nm was observed, consistent with the literature value.

Detection of NFK in γ -WLB_U2

The assay used to detect NFK in γ -WLB_U2 was based from Tomek et al (Figure 18).²³ Briefly, NFK is reacted with piperidine to synthesize NFK-PIP, which fluoresces at 500 nm when excited at 400 nm.²³ The native and irradiated WLB_U2 and WLB_U2-PIP solutions at excitation wavelengths of 330 and 400 nm are shown in Figure 19. NFK has a reported maximum fluorescence at 400 nm when excited at 330 nm.³¹ A similar fluorescence was observed in γ -WLB_U2 (Figure 19A). This spectrum is also consistent with a complete loss of the indole structure because tryptophan does not give emission between 350 nm to 500 nm at the same excitation wavelength. Additionally, NFK-PIP has a peak emission wavelength of 500 nm when excited at 400 nm²³, which was also present in the γ -WLB_U2-PIP solution (Figure 19B). Although there was no positive control for this assay because the synthesized NFK could not be confirmed, the data is not inconsistent with the presence of NFK in γ -WLB_U2, suggesting that the tryptophan residues may have oxidized into NFK upon irradiation.

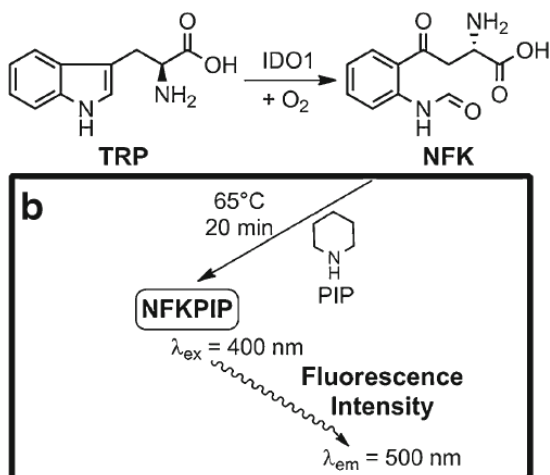


Figure 18. Reaction scheme of the NFKPIP fluorescence assay.²³

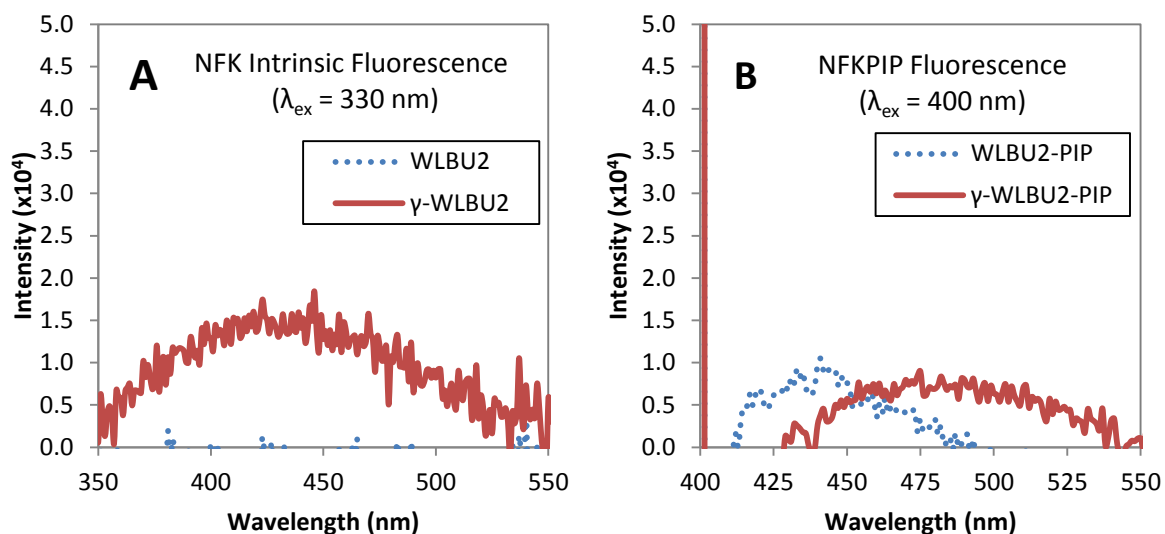


Figure 19. Fluorescence spectra of native and irradiated (A) WLBU2 and (B) WLBU2-PIP solutions at excitation wavelengths 330 nm and 400 nm, respectively. NFK has a characteristic emission peak at 400 nm when excited at 330 nm. NFK-PIP has a reported peak at 500 nm when excited at 400 nm. Water peak at approximately 400 nm was not suppressed.

Mass spectrometry of peptides

The low-resolution mass spectrum of 0.3 mg/mL native WLBU2 in water is shown in Figure 20 and 1.0 mg/mL γ -WLBU2 in Figure 21. The expected molecular weight of 3400.1 Da for native WLBU2 was consistent with the native spectrum, which has a base peak intensity (BPI) at 3399.1 m/z (Figure 17). However, γ -WLBU2 displayed a lower BPI of 3370.2 m/z, which is not consistent with an expected higher BPI of approximately 3496.1 m/z for NFK, although the broad peak is difficult to interpret. Even if water loss was factored in, the corrected BPI would be at 3388.2 m/z, which is close to the molecular weight of native WLBU2 and does not confirm oxidation of the tryptophan residues into NFK. However, the spectrum also displayed many peaks around the area of interest that had similar BPI, perhaps indicating that a small percentage of tryptophan residues in γ -WLBU2 were oxidized into NFK, which is consistent with previous

research.¹⁸ Based on the noisy, low-resolution mass spectrum of γ -WLBU2, the formation of NFK cannot be confirmed from this data.

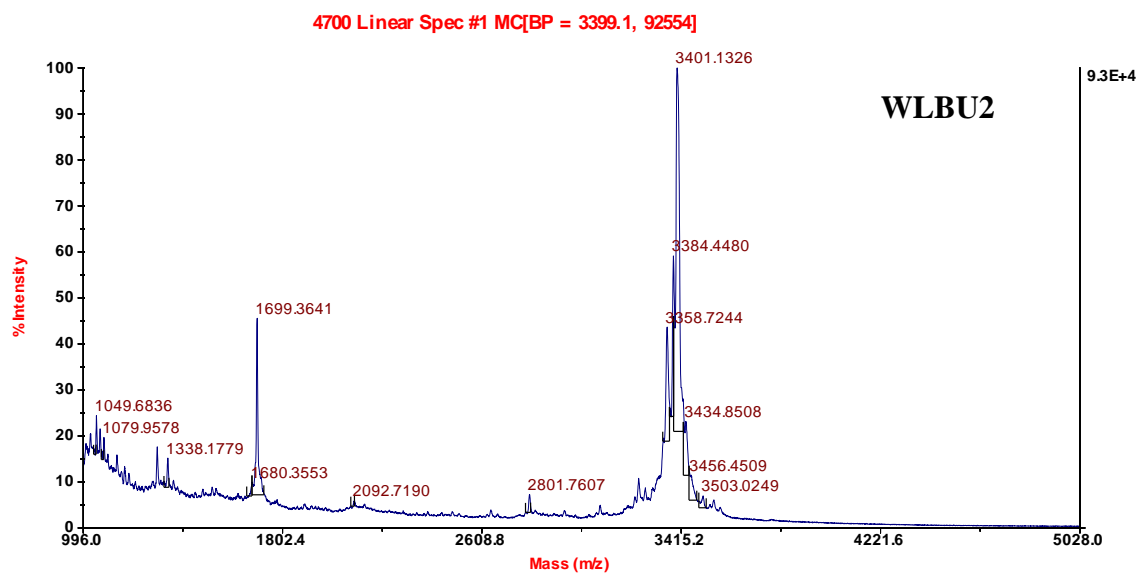


Figure 20. Low resolution mass spectrum of 0.3 mg/mL WLBU2.

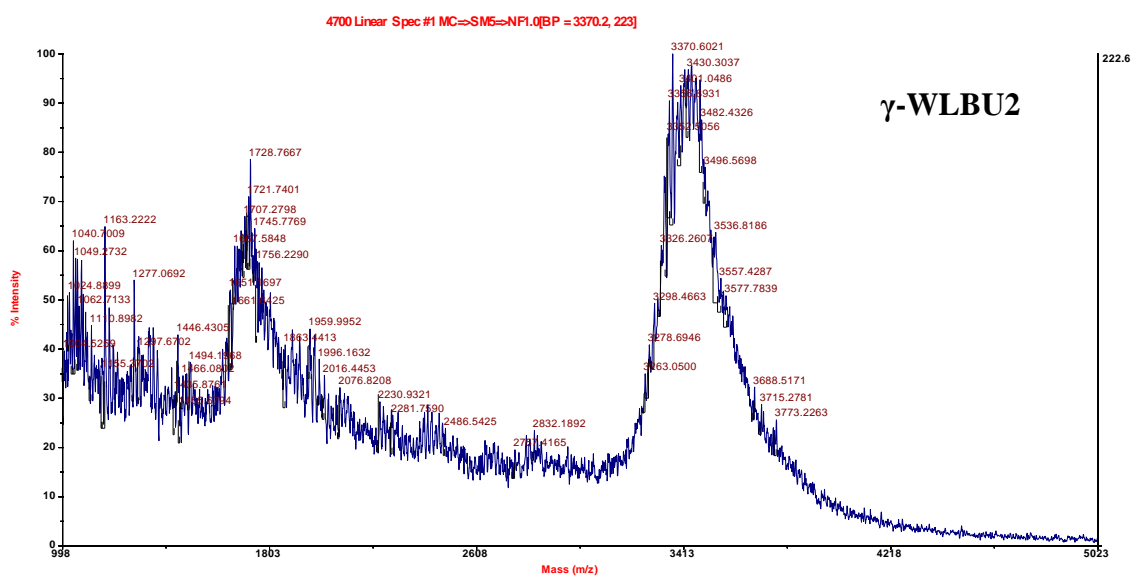


Figure 21. Low-resolution mass spectrum of 1.0 mg/mL γ -WLBU2.

Antimicrobial Activity

Figure 22 shows the inhibition of bacterial growth of *E. coli* and *P. pentosaceus* corresponding to the labeling in Table 2. All peptide samples inhibited bacterial growth. Inhibition zones (Figure 23) caused by γ -WLBU2 were more defined against *P. pentosaceus*, suggesting that irradiation may slightly increase WLBU2 antimicrobial activity against Gram-positive bacteria, although future research is necessary to support this claim. Image analysis of the inhibition zones yielded many significant differences between treatments ($p < 0.01$), but the differences may not be important.

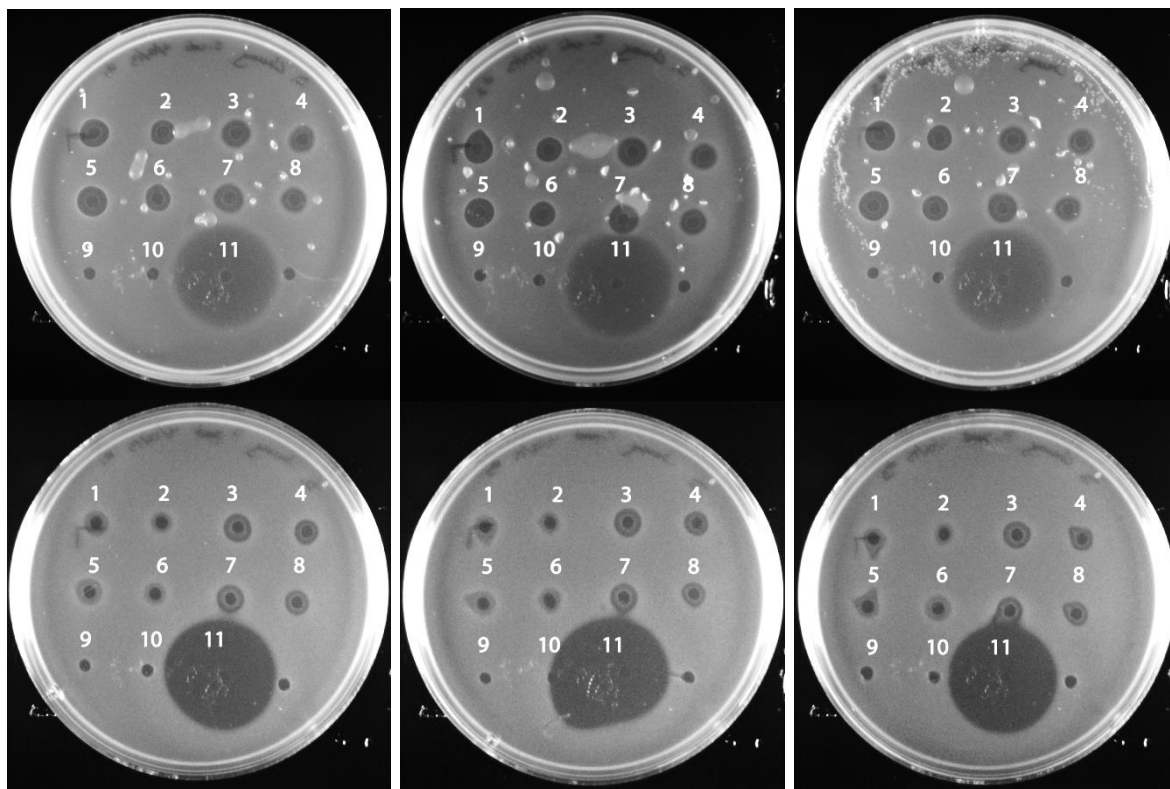


Figure 22. Radial diffusion bacterial inhibition assay results of *E. coli* (top row) and *P. pentosaceus* (bottom row). Numbering scheme corresponds to Table 2.

Table 2. List of solutions and concentrations used for the radial diffusion bacterial inhibition assay.

| Number | Solution | |
|--------|---------------------------|------------------|
| 1 | 1.0 mg/mL WLBu2 | H ₂ O |
| 2 | 0.5 mg/mL WLBu2 | |
| 3 | 1.0 mg/mL γ -WLBu2 | |
| 4 | 0.5 mg/mL γ -WLBu2 | |
| 5 | 1.0 mg/mL WLBu2 | D ₂ O |
| 6 | 0.5 mg/mL WLBu2 | |
| 7 | 1.0 mg/mL γ -WLBu2 | |
| 8 | 0.5 mg/mL γ -WLBu2 | |
| 9 | D ₂ O | |
| 10 | H ₂ O | |
| 11 | 50 mg/mL ampicillin | |

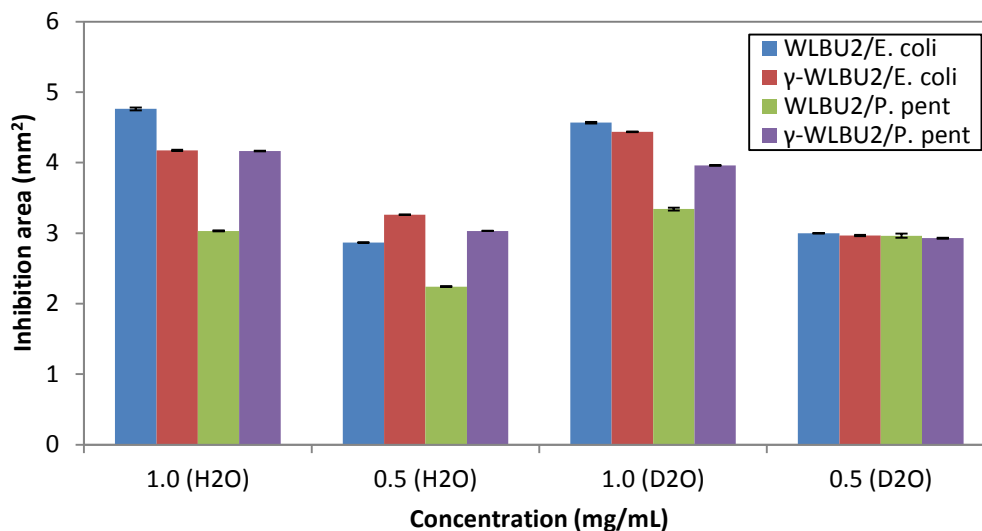


Figure 23. Mean diameter of WLBU2 kill zones against *E. coli* and *P. pentosaceus*. A small effect of concentration was observed. Deuterated water (D₂O) had no effect on bacterial inhibition, with or without WLBU2 peptide. Error bars represent 95% confidence interval (N = 3).

Higher tryptophan content and α -helicity generally increases CAP activity^{6,7}, yet the irradiated peptide appears to have lost some or all of the tryptophan indole side chains and exhibits decreased α -helix conformation. Despite these structural changes, WLBU2 remained effective against Gram-positive and Gram-negative bacteria after irradiation. ¹H-NMR, UV, and intrinsic tryptophan fluorescence data are consistent with oxidation of tryptophan side chains. This somewhat decreases the hydrophobicity of γ -WLBU2 and alters the stability of the α -helix conformation in the presence of perchlorate ions. The decrease in α -helicity may not affect the peptide's ability to disrupt bacterial membrane. Wu et al. has recently shown that peptides with partial α -helicity undergo an increase in helicity after entry into a PEO brush layer³⁵, which is likely due to decreased capacity for peptide-hydrogen bonding in the brush environment. Similarly, the γ -WLBU2, which has lower α -helicity than native WLBU2, may increase its α -helical conformation upon integration into the cell membrane.

Conclusions and Future Recommendations

The aim of this work was to characterize effects of γ -irradiation on WLBU2 to assess the feasibility of using γ -irradiation to immobilize WLBU2-PEO/PBD/PEO triblock constructs on polymer medical device surfaces for the treatment of sepsis. Analysis via $^1\text{H-NMR}$, UV, fluorescence, and CD spectroscopies show that γ -WLBU2 spectra are different from native WLBU2, indicating structural and chemical changes upon irradiation. The absence of NMR peaks in γ -WLBU2 associated with the indole structure suggests a ring-opening of tryptophan via oxidation in WLBU2. Furthermore, UV and fluorescence spectroscopies showed the absence of peaks associated with tryptophan, also suggesting that irradiation causes chemical changes on the tryptophan side chains of WLBU2. The CD spectra showed lower α -helicity in γ -WLBU2, which is consistent with structural changes caused by oxidation of tryptophan into more polar side chains (e.g. NFK), which lowered the stability of α -helices in presence of perchlorate ions. However, the prediction of tryptophan oxidizing into NFK upon irradiation could not be confirmed from the PIP fluorescence assay, mass spectrometry, or UV spectroscopy. Although a decrease in tryptophan content and α -helicity is observed, γ -WLBU2 remains at least as effective as native WLBU2 against Gram-positive and Gram-negative bacteria.

Future experiments should aim to elucidate the structural change of γ -WLBU2, especially confirmation of NFK formation. This could be achieved by performing a high-resolution mass spectrometry using a higher-concentration sample and verifying that NFK was the major product of synthesis to use as a positive control. Elucidation of γ -irradiated peptide will provide insight on other compounds (i.e. unnatural amino acids)

that might replace tryptophan while maintaining high α -helicity, giving more options and flexibility for engineering CAPs. Additionally, this could open up the possibility to mass produce the peptide in mammalian or insect cell cultures in an industrial setting to lower production cost of the peptide. Furthermore, the antimicrobial and endotoxin-binding activity of immobilized γ -WLBU2 attached to surfaces via irradiation remains to be analyzed. One method would be to perform surface analysis (e.g. optical waveguide lightmode spectroscopy, scanning electron microscopy, and quartz-crystal microbalance with dissipation (QCM-D)) to observe bacteria and endotoxin binding to the peptide-coated surfaces. In addition, future work must demonstrate that γ -irradiation of WLBU2 does not change the native peptide's lack of cytotoxicity to mammalian cells.

This study has shown that γ -irradiation alters the structure of WLBU2, but the antimicrobial activity was not adversely affected. Therefore, the data indicates that γ -irradiation is viable method to immobilize WLBU2-triblock constructs onto polymer biomedical surfaces without adversely affecting antimicrobial activity of the peptide.

References

- 1 Czura, C. J. “Merinoff Symposium 2010: Sepsis”—Speaking with One Voice. *Molecular Medicine* **17**, 2 (2011).
- 2 Hancock, R. E. & Sahl, H.-G. Antimicrobial and host-defense peptides as new anti-infective therapeutic strategies. *Nature biotechnology* **24**, 1551-1557 (2006).
- 3 Cohen, J. The immunopathogenesis of sepsis. *Nature* **420**, 885-891 (2002).
- 4 Wood, K. A. & Angus, D. C. Pharmacoeconomic implications of new therapies in sepsis. *Pharmacoeconomics* **22**, 895-906 (2004).
- 5 Rollins-Smith, L. A. *et al.* Antimicrobial peptide defenses against pathogens associated with global amphibian declines. *Developmental & Comparative Immunology* **26**, 63-72, doi:[http://dx.doi.org/10.1016/S0145-305X\(01\)00041-6](http://dx.doi.org/10.1016/S0145-305X(01)00041-6) (2002).
- 6 Deslouches, B. *et al.* Activity of the De Novo Engineered Antimicrobial Peptide WLBU2 against *Pseudomonas aeruginosa* in Human Serum and Whole Blood: Implications for Systemic Applications. *Antimicrobial Agents and Chemotherapy* **49**, 3208-3216, doi:10.1128/aac.49.8.3208-3216.2005 (2005).
- 7 Deslouches, B. *et al.* De Novo Generation of Cationic Antimicrobial Peptides: Influence of Length and Tryptophan Substitution on Antimicrobial Activity. *Antimicrobial Agents and Chemotherapy* **49**, 316-322, doi:10.1128/aac.49.1.316-322.2005 (2005).
- 8 Gonzalez, I. A. *et al.* Peptides as potent antimicrobials tethered to a solid surface: Implications for medical devices. *Nature Precedings* (2008).
- 9 Amiji, M. & Park, K. Prevention of protein adsorption and platelet adhesion on surfaces by PEO/PPO/PEO triblock copolymers. *Biomaterials* **13**, 682-692, doi:[http://dx.doi.org/10.1016/0142-9612\(92\)90128-B](http://dx.doi.org/10.1016/0142-9612(92)90128-B) (1992).
- 10 Drury, J. L. & Mooney, D. J. Hydrogels for tissue engineering: scaffold design variables and applications. *Biomaterials* **24**, 4337-4351, doi:[http://dx.doi.org/10.1016/S0142-9612\(03\)00340-5](http://dx.doi.org/10.1016/S0142-9612(03)00340-5) (2003).
- 11 Halperin, A. Polymer Brushes that Resist Adsorption of Model Proteins: Design Parameters. *Langmuir* **15**, 2525-2533, doi:10.1021/la981356f (1999).
- 12 Li, J.-T., Carlsson, J., Lin, J.-N. & Caldwell, K. D. Chemical modification of surface active poly (ethylene oxide)-poly (propylene oxide) triblock copolymers. *Bioconjugate chemistry* **7**, 592-599 (1996).
- 13 Neff, J., Caldwell, K. & Tresco, P. A novel method for surface modification to promote cell attachment to hydrophobic substrates. *Journal of biomedical materials research* **40**, 511-519 (1998).
- 14 McPherson, T. B., Shim, H. S. & Park, K. Grafting of PEO to glass, nitinol, and pyrolytic carbon surfaces by γ irradiation. *Journal of biomedical materials research* **38**, 289-302 (1997).
- 15 Fry, A. K., Schilke, K. F., McGuire, J. & Bird, K. E. Synthesis and anticoagulant activity of heparin immobilized “end-on” to polystyrene microspheres coated with end-group activated polyethylene oxide. *Journal of Biomedical Materials Research Part B: Applied Biomaterials* **94B**, 187-195, doi:10.1002/jbm.b.31640 (2010).

- 16 Levin, C. H. & Bobrowski, K. The use of the methods of radiolysis to explore the mechanisms of free radical modifications in proteins. *Journal of proteomics* (2013).
- 17 Xu, G. & Chance, M. R. Radiolytic modification and reactivity of amino acid residues serving as structural probes for protein footprinting. *Analytical chemistry* **77**, 4549-4555 (2005).
- 18 Wickern, B. v., Müller, B., Simat, T. & Steinhart, H. Determination of γ -radiation induced products in aqueous solutions of tryptophan and synthesis of 4-, 6- and 7-hydroxytryptophan. *Journal of Chromatography A* **786**, 57-65, doi:[http://dx.doi.org/10.1016/S0021-9673\(97\)00516-5](http://dx.doi.org/10.1016/S0021-9673(97)00516-5) (1997).
- 19 Rifkind, J. M. Helix - coil transition of poly - L - arginine: A comparison with other basic polypeptides. *Biopolymers* **8**, 685-688 (1969).
- 20 Whitmore, L. & Wallace, B. A. DICHROWEB, an online server for protein secondary structure analyses from circular dichroism spectroscopic data. *Nucleic Acids Research* **32**, W668-W673, doi:10.1093/nar/gkh371 (2004).
- 21 Whitmore, L. & Wallace, B. A. Protein secondary structure analyses from circular dichroism spectroscopy: Methods and reference databases. *Biopolymers* **89**, 392-400, doi:10.1002/bip.20853 (2008).
- 22 Ehrenshaft, M. *et al.* Immunological detection of N-formylkynurenine in oxidized proteins. *Free Radical Biology and Medicine* **46**, 1260-1266 (2009).
- 23 Tomek, P. *et al.* Formation of an N-formylkynurenine-derived fluorophore and its use for measuring indoleamine 2,3-dioxygenase 1 activity. *Anal Bioanal Chem* **405**, 2515-2524, doi:10.1007/s00216-012-6650-y (2013).
- 24 Shamova, O. *et al.* ChBac3.4: A Novel Proline-Rich Antimicrobial Peptide from Goat Leukocytes. *Int J Pept Res Ther* **15**, 31-42, doi:10.1007/s10989-008-9159-7 (2009).
- 25 NIH. *ImageJ - Image Processing and Analysis in Java*, <<http://rsbweb.nih.gov/ij/index.html>> (2013).
- 26 AIST. *Spectral Database for Organic Compounds SDBS*, <<http://sdb.srioddb.aist.go.jp>> (2013).
- 27 Wishart, D. S. *et al.* HMDB 3.0--The Human Metabolome Database in 2013. *Nucleic Acids Res* **41**, D801-807, doi:10.1093/nar/gks1065 (2013).
- 28 Wishart, D. S. *et al.* HMDB: a knowledgebase for the human metabolome. *Nucleic Acids Res* **37**, D603-610, doi:10.1093/nar/gkn810 (2009).
- 29 Wishart, D. S. *et al.* HMDB: the Human Metabolome Database. *Nucleic Acids Res* **35**, D521-526, doi:10.1093/nar/gkl923 (2007).
- 30 Talrose, V. *et al.* *UV/Visible Spectra*.
- 31 Pirie, A. Fluorescence of N'-formylkynurenine and of protein exposed to sunlight. *Biochemical Journal* **128**, 1365 (1972).
- 32 Prah, S. *Tryptophan*, <<http://omlc.org.edu/spectra/PhotochemCAD/html/091.html>> (2012).
- 33 Du, H., Fuh, R.-C. A., Li, J., Corkan, L. A. & Lindsey, J. S. PhotochemCAD \ddagger : A Computer-Aided Design and Research Tool in Photochemistry. *Photochemistry and Photobiology* **68**, 141-142, doi:10.1111/j.1751-1097.1998.tb02480.x (1998).
- 34 Dixon, J. M., Taniguchi, M. & Lindsey, J. S. PhotochemCAD 2: A Refined Program with Accompanying Spectral Databases for Photochemical Calculations \S .

- Photochemistry and Photobiology* **81**, 212-213, doi:10.1111/j.1751-1097.2005.tb01544.x (2005).
- 35 Wu, X., Ryder, M. P., McGuire, J. & Schilke, K. F. Adsorption, structural alteration and elution of peptides at pendant PEO layers. *Colloids and Surfaces B: Biointerfaces*, doi:10.1016/j.colsurfb.2013.07.033 (2013).
- 36 Ascitutto, E. K., General, I. J., Xiong, K., Asher, S. A. & Madura, J. D. Sodium Perchlorate Effects on the Helical Stability of a Mainly Alanine Peptide. *Biophysical Journal* **98**, 186-196, doi:<http://dx.doi.org/10.1016/j.bpj.2009.10.013> (2010).
- 37 Greenfield, N. J. Using circular dichroism spectra to estimate protein secondary structure. *Nature protocols* **1**, 2876-2890 (2007).
- 38 Kurnasov, O. *et al.* NAD Biosynthesis: Identification of the Tryptophan to Quinolate Pathway in Bacteria. *Chemistry & Biology* **10**, 1195-1204, doi:<http://dx.doi.org/10.1016/j.chembiol.2003.11.011> (2003).
- 39 Ronsein, G. E., de Oliveira, M. C. B., de Medeiros, M. H. G. & Di Mascio, P. Characterization of O₂ (1Δg)-derived oxidation products of tryptophan: A combination of tandem mass spectrometry analyses and isotopic labeling studies. *Journal of the American Society for Mass Spectrometry* **20**, 188-197 (2009).
- 40 Kasson, T. M. D. & Barry, B. A. Reactive oxygen and oxidative stress: N-formyl kynurenine in photosystem II and non-photosynthetic proteins. *Photosynthesis research* **114**, 97-110 (2012).

Appendices

Appendix I – Reference $^1\text{H-NMR}$ Spectra

All reference $^1\text{H-NMR}$ spectra and peak assignments of arginine, tryptophan, and valine are listed in Figures AI 1 – AI 4 and were taken from National Institute of Advanced Industrial Science and Technology (AIST) spectral database and the Human Metabolome Database.²⁶⁻²⁹

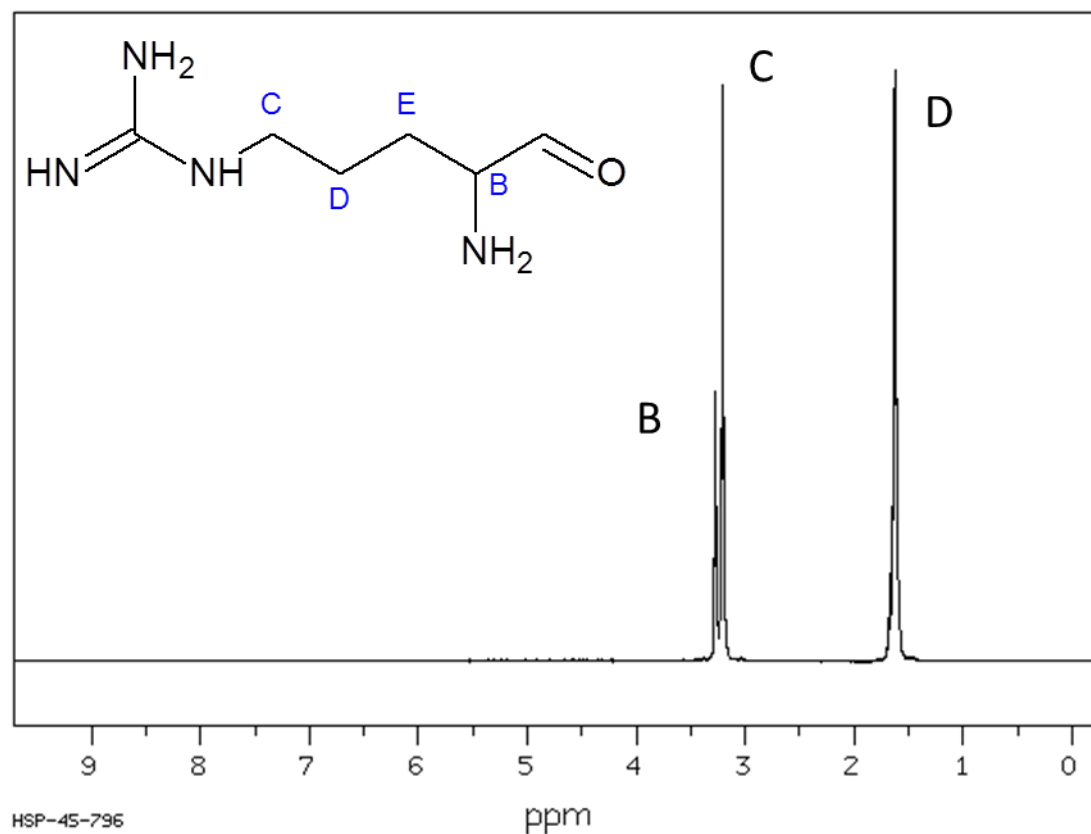


Figure AI 1. Reference $^1\text{H-NMR}$ spectrum of L-arginine in D_2O with peak assignments.

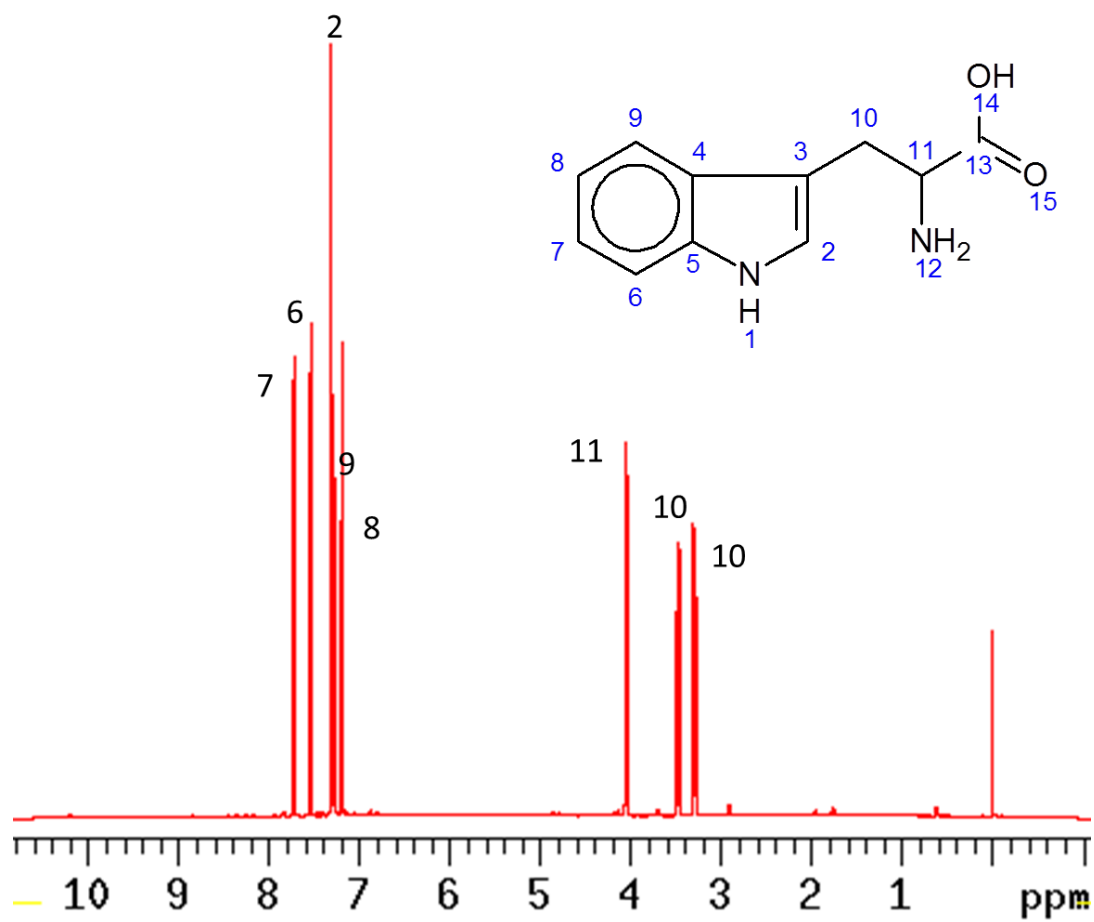


Figure AI 2. Reference ¹H-NMR spectrum of L-tryptophan in H₂O with peak assignments.

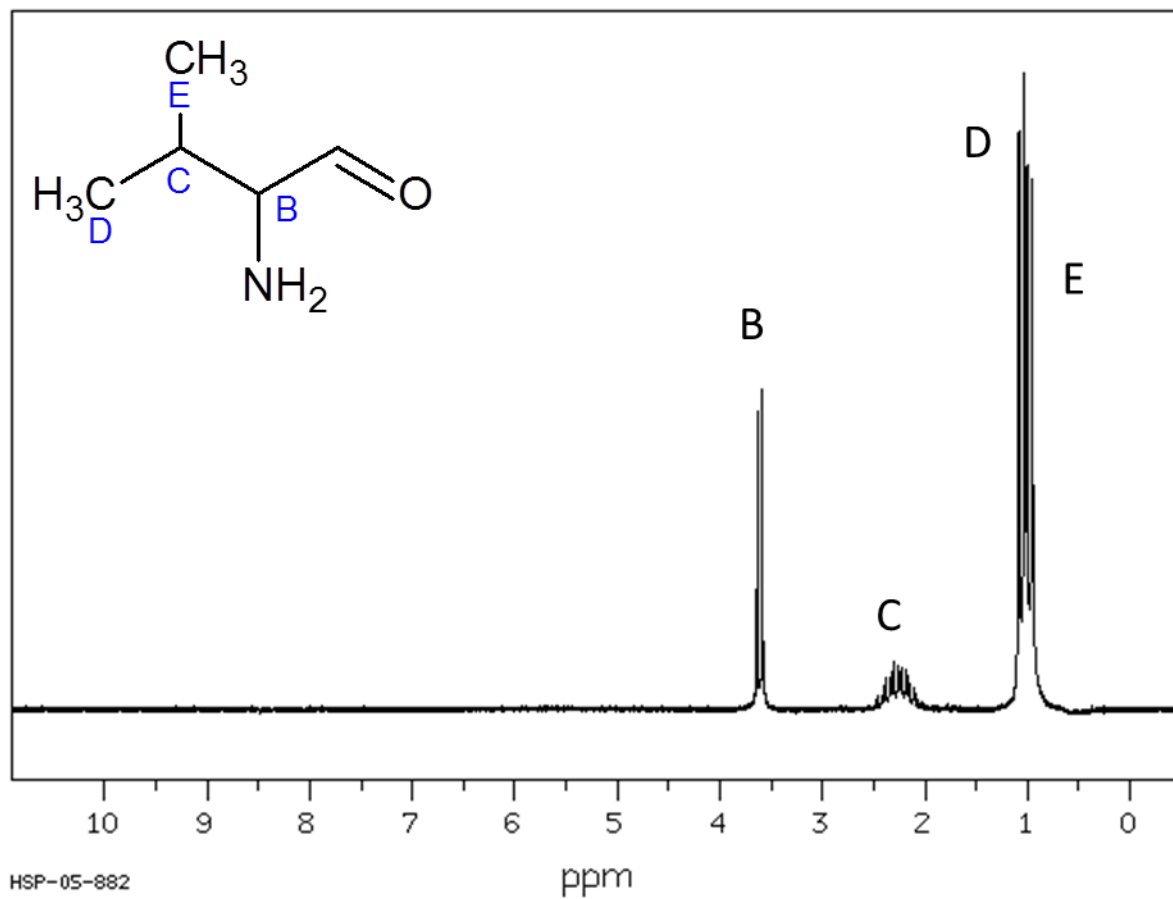


Figure AI 3. Reference ¹H-NMR spectrum of DL-valine in D₂O with peak assignments.

Appendix II – Radial diffusion inhibition assay plating recipe***E. coli***Underlayer without 100 mM NaCl

60 mg Trypticase Soy Broth (0.3 mg/mL)
20 mL 0.1 M sodium phosphate buffer, pH 7.4
2 g agarose
ddH₂O to 200 mL

Underlayer with 100 mM NaCl

60 mg Trypticase Soy Broth (0.3 mg/mL)
20 mL 0.1 M sodium phosphate buffer, pH 7.4
20 mL 1 M NaCl
2 g agarose
ddH₂O to 200 mL

Overlayer

12 g Trypticase Soy Broth (60 mg/mL)
20 mL 0.1 M sodium phosphate buffer, pH 7.4
2 g agarose
ddH₂O to 200 mL

P. pentosaceusUnderlayer without 100 mM NaCl

60 mg MRS Broth (0.3 mg/mL)
20 mL 0.1 M sodium phosphate buffer, pH 7.2
2 g agarose
ddH₂O to 200 mL

Underlayer with 100 mM NaCl

60 mg MRS Broth (0.3 mg/mL)
20 mL 0.1 M sodium phosphate buffer, pH 7.2
20 mL 1 M NaCl
2 g agarose
ddH₂O to 200 mL

Overlayer

12 g MRS Broth (60 mg/mL)
20 mL 0.1 M sodium phosphate buffer, pH 7.2
2 g agarose
ddH₂O to 200 mL

All solutions were autoclaved for 30 minutes before plating.

University Honors College Copyright Release Form

We are planning to release this Honors Thesis in one or more electronic forms. I grant the right to publish **my thesis / my abstract (circle one)** entitled,

Structural and activity characterization of irradiated antimicrobial peptide (WLBU2) for use in blood processing and biomedical applications, in the Honors College OSU Library's Digital Repository (D-Space), and its employees the nonexclusive license to archive and make accessible, under conditions specified below.

The right extends to any format in which this publication may appear, including but not limited to print and electronic formats. Electronic formats include but are not limited to various computer platforms, application data formats, and subsets of this publication. I, as the Author, retain all other rights to my thesis, including the right to republish my thesis all or part in other publications.

I certify that all aspects of my thesis which may be derivative have been properly cited, and I have not plagiarized anyone else's work. I further certify that I have proper permission to use any cited work which is included in my thesis which exceeds the Fair Use Clause of the United States Copyright Law, such as graphs or photographs borrowed from other articles or persons.

Signature: _____

Printed Name: _____

Date: _____